Electronic Supplementary Material (ESI) for Journal of Materials Chemistry A.

Electronic Supplementary Information

Visualization and monitoring of dynamic damaging-healing processes of polymers by AIEgen-loaded multifunctional microcapsules

Shusheng Chen,[abcd] Ting Han,*[a] Junkai Liu,[e] Xinting Liang,[f] Jinglei Yang*[bc] and Ben Zhong Tang*[eg]

[a]Center for AIE Research, Shenzhen Key Laboratory of Polymer Science and Technology, Guangdong Research Center for Interfacial Engineering of Functional Materials, College of Materials Science and Engineering, Shenzhen University, Shenzhen 518060, China

[b]Department of Mechanical and Aerospace Engineering, The Hong Kong University of Science and Technology, Clear Water Bay, Hong Kong SAR, China

[e]HKUST Shenzhen-Hong Kong Collaborative Innovation Research Institute, Futian, Shenzhen 518048, China

[d]School of Chemistry and Environmental Engineering, Hanshan Normal University, Chaozhou, Guangdong 521041, China

[e]Department of Chemistry, Hong Kong Branch of Chinese National Engineering Research Center for Tissue Restoration and Reconstruction, The Hong Kong University of Science and Technology, Clear Water Bay, Kowloon, Hong Kong, China

[f]Key Laboratory of Bioorganic Chemistry and Molecular Engineering of Ministry of Education and Beijing National Laboratory for Molecular Science, and Peking-Tsinghua Center for Life Sciences, Peking University, Beijing, 100871, China.

[g]School of Science and Engineering, Shenzhen Institute of Aggregate Science and Technology, The Chinese University of Hong Kong, Shenzhen, Guangdong 518172, China

Table of Contents

1. Experimental Section

Materials and methods: Three TICT-type AIEgens, dimethoxy-tetraphenylethene-(*Z*)-4-benzylidene-2-methyloxazol-5(4H)-one (DMTPE-BMO), triphenylamine-(*Z*)-4-benzylidene-2-methyloxazol-5(4H)-one (TPA-BMO), and tetraphenylethene-(*Z*)-4-benzylidene-2-methyloxazol-5(4H)-one (TPE-BMO) were synthesized according to the literature methods.[1, 2] 4,4-Diphenylmethane diisocyanate (MDI) prepolymer Suprasec 2644 was obtained from Huntsman. Hexamethylene diisocyanate (HDI), tetraethylenepentamine (TEPA), polyvinyl alcohol (PVA), glycidylmethacrylate (GMA), hydroxyphenethylamine hydrochloride (dopamine), and tris-(hydroxymethyl) aminomethane (TRIS) were purchased from Sigma-Aldrich. Epolam 5015 and hardener 5015 were supplied by Axson. All chemical reagents were used as received and without further purification. The electronic structures and potential energy surfaces in the excited state of TPE-BMO were calculated at TD-B3LYP/6-31G(d,p) level. The SMD model was applied for the simulation in the solution. The TPE-BMO in the crystal was calculated with the combined quantum mechanics and molecular mechanics (QM/MM) method using the ONIOM model. We constructed the ONIOM model by cutting a cluster from the crystal. The central molecule was treated as the QM part at TD-B3LYP/6-31G(d,p) level and the surrounding ones acted as the MM part with the universal force field.

Fluorescence characterization: Photoluminescence (PL) spectra were obtained via a Horiba Fluorolog spectrophotometer. The time-dependent fluorescence spectra for tracking the reaction between HDI and water were recorded by placing the sample in a heating holder at 60 ℃. Fluorescence quantum yields (Φ_F) were measured by a Hamamatsu absolute photoluminescence quantum yield spectrometer C11347 Quantaurus QY. UV-vis spectra were obtained via a PerkinElmer Lambda 365 UV/Vis spectrophotometer. Real-time fluorescent images were collected by a digital camera (Canon EOS 60D) with a self-timer (Figure S4). The sample, the mixture of HDI and water, was put on a hotplate at 60 ℃ in a dark room. The UV lamp was connected with an intelligent socket that can be controlled by a smartphone. MATLAB program was used to transform the RGB color space to grayscale intensity, and CIE x and y chromaticity values.

Preparation of microcapsules (MCs): Multi-layered microcapsules containing the HDI solution of TICT-type AIEgen were synthesized via interfacial polymerization and repeated dopamine self-polymerization. In the first step, the oil-phase mixture of 1 g of Suprasec 2644 and 8 g of AIEgen/HDI solution (0.5 wt%) was added dropwise into 50 mL of PVA aqueous solution (1 wt%) under agitation rate of 400 rpm for 15 min followed by the addition of 1 g of TEPA to initiate the interfacial polymerization. The reaction temperature was raised to 40 ℃ for 3 h. The obtained polyurea (PU) MCs were rinsed with deionized water several times, and then added to 50 mL of TRIS buffer solution (pH 8.5). After the addition of 2.5 g of dopamine, the mixture was stirred at a rate of 200 rpm at room temperature for 12 h to deposit a layer of polydopamine (PDA) shell via the self-polymerization of dopamine. This dopamine self-polymerization process was repeated four times to deposit multiple PDA layers on the surface of MCs. The resulting MCs were denoted as 1PDA/PU MCs, 2PDA/PU MCs, 3PDA/PU MCs, and 4PDA/PU MCs.

Characterization of MCs: Scanning electron microscopy (JEOL-6390) was applied to characterize the morphologies of MCs. Fourier transform infrared (FTIR) spectra were recorded on a Bruker Vertex 70 FTIR spectrometer. Thermogravimetric analysis (TGA) was carried under nitrogen atmosphere with a TA Q5000 thermal analyzer from 25 to 800 ℃ at a heating rate of 20 ℃/min. The core fractions of MCs were roughly estimated from the TGA results. The mechanical properties of MCs were measured using a single capsule compression machine at a loading rate of 2 μm/s. The nominal stress was defined as the load divided by the maximum cross-sectional area of the MC. The nominal strain was defined as the displacement divided by the diameter of the MC. Photographs of MCs were taken by a digital camera (Canon EOS 60D) under ambient room lighting and illumination with a hand-held Spectroline ENF-260C UV lamp (365 nm). Fluorescent images of individual MCs were captured using an Olympus BX41 fluorescence microscope under a bright field and excitation wavelength of 460–490 nm (dichroic mirror = 600 nm and emission filter = 610 nm). Stereomicroscopic images of intact and broken MCs were acquired using a Motic Moticam 1080 microscope under ambient room lighting and 365 nm UV illumination with a hand-held lamp. The mean diameter and size distribution of the 4PDA/PU MCs measured and analyzed from SEM images of at least 200 individual microcapsules by using ImageJ.

Preparation of MC-embedded epoxy coatings: Epoxy (EP) resin (Epolam 5015) was firstly mixed with its hardener before adding 15 wt% of MCs. After degassing in a vacuum oven for 20 min, the mixture was coated onto substrates with different shapes, including quartz glass, aluminized paper, and packaging box. After a complete cure at room temperature, the final thickness of the coating was around 400 μm. Pure epoxy coatings were prepared following the same procedure as for the controls.

Monitoring of the healing process of MC-embedded EP coatings: To track the healing process of the MC-embedded EP coating, the coatings were firstly scratched with a razor blade, and then a digital camera (Canon EOS 60D) with a self-timer was used to take real-time fluorescent images. UV-vis spectra of the MC-embedded EP coating and pure EP coating were obtained via a Lambda 950 UV/vis spectrophotometer. The Tyndall effect was performed in silica sol with and without an MC-embedded EP coating shelter, and a laser pointer pen (635 nm) was used as the light source. Scanning electron microscopy (JEOL-6390) was applied to observe the cracks of coatings.

Water permeation test: The water permeation test was conducted using a homemade device.[3] It consists of a water container, a clamp, and a water collector. The through-thickness cracks with a length of 10 mm and a width of 50 μm were introduced to the coated aluminized papers by cutting with a sharp blade. The sample was clamped between the water container and the collector. Paraffin film was used to ensure good sealability. During the test, 50 g of water was added to the container. After 10 minutes, the weight of penetrated water was recorded.

Characterization of MC-embedded EP packaging coatings in boxes: Packaging coatings were prepared by covering pure EP coating and MC-embedded EP coating on the bottom side of thin plastic boxes, respectively. To test the UV-blocking function of the MC-embedded EP coating, the boxes containing commercially available photosensitive powder were placed under sunlight for 5 min. Then, they were transferred indoors and opened to check the state of powder. To test the self-healing and water-protective abilities of the MC-embedded EP coating, a through-thickness crack with a length of 3 mm and a width of 50 μm was introduced to the coating by cutting with a sharp blade. Subsequently, the box was soaked into the water for 1 min and pressed manually. After drying the outer surface of the box, it was placed on a hotplate at 70 ℃ for 10 min to make sure that the permeated water caused the inside upper surface of the box to steam up.

Supporting References

1. Zhang, Y, Jiang, M, Han, T, *et al.* Aggregation-induced emission luminogens as color converters for visible-light communication. *ACS Appl. Mater. Interfaces*, 2018; **10**: 34418-26.
2. Jiang, M, He, Z, Zhang, Y, *et al.* Development of benzylidene-methyloxazolone based AIEgens and decipherment of their working mechanism. *J. Mater. Chem. C*, 2017; **5**: 7191-9.
3. Zhang, H, Chong, YB, Zhao, Y, *et al.* Self-Sealing Polyolefin by Super-Absorbent Polymer. *Eng. Sci.*, 2019; **8**: 66-75.

2. Supplementary Figures

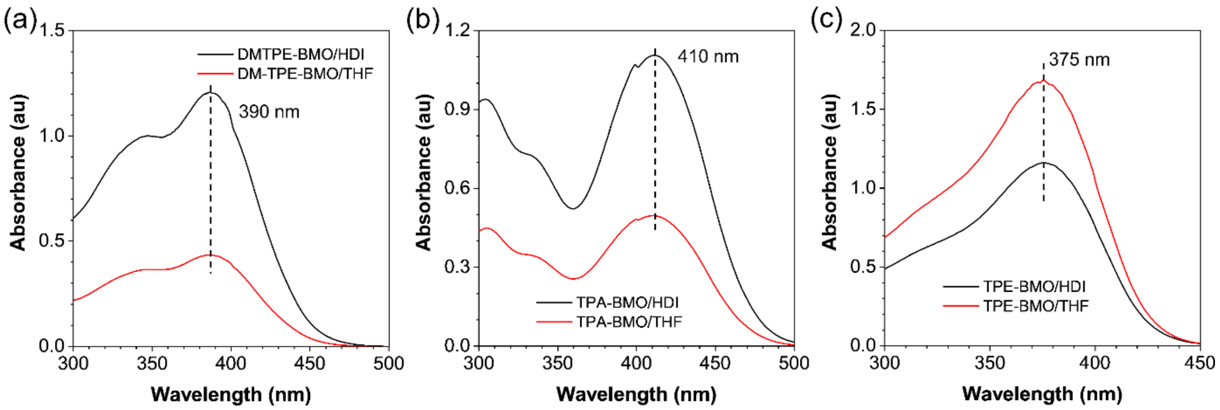

Figure S1. UV-vis absorption spectra of (a) DMTPE-BMO/HDI and DMTPE-BMO/THF solutions, (b) TPA-BMO/HDI and TPA-BMO/THF solutions, and (c) TPE-BMO/HDI and TPE-BMO /THF solutions.

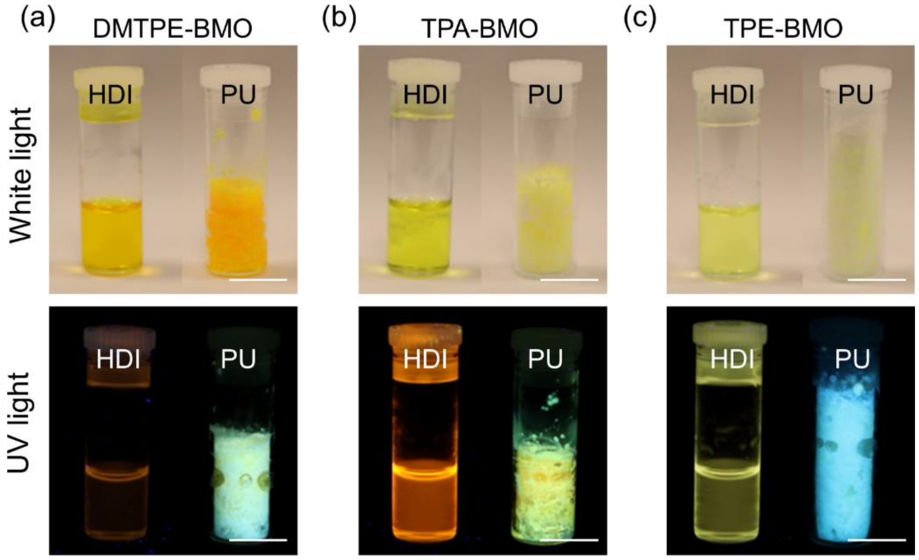

Figure S2. Photographs of (a) DMTPE-BMO, (b) TPE-BMO, and (c) TPA-BMO in HDI solutions and the corresponding PU solid states taken under room light and 365 nm UV light illumination. The scale bar indicates 10 mm.

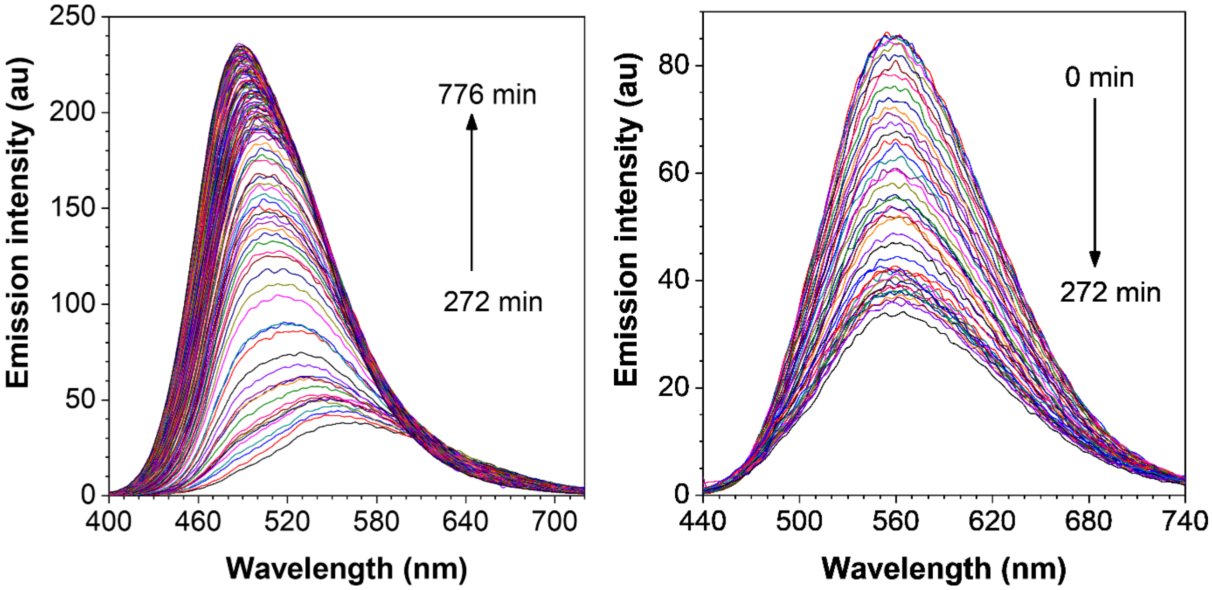

Figure S3. Time-dependent PL spectra of the TPE-BMO during the curing reaction of HDI with water.

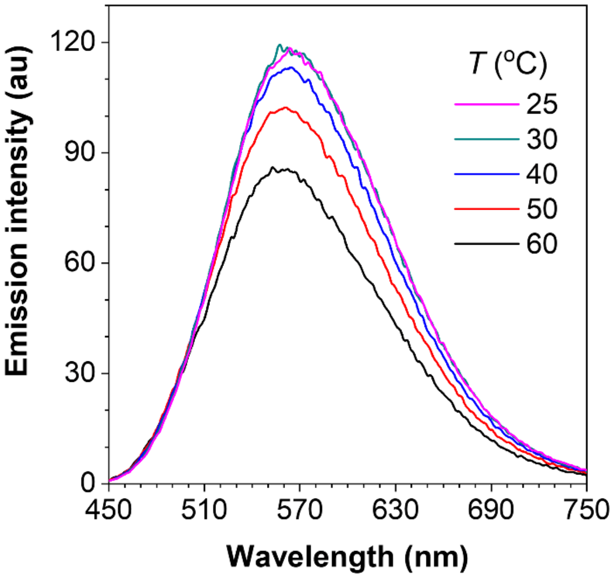

Figure S4. Temperature-dependent PL spectra of the TPE-BMO during the curing reaction of HDI with water.

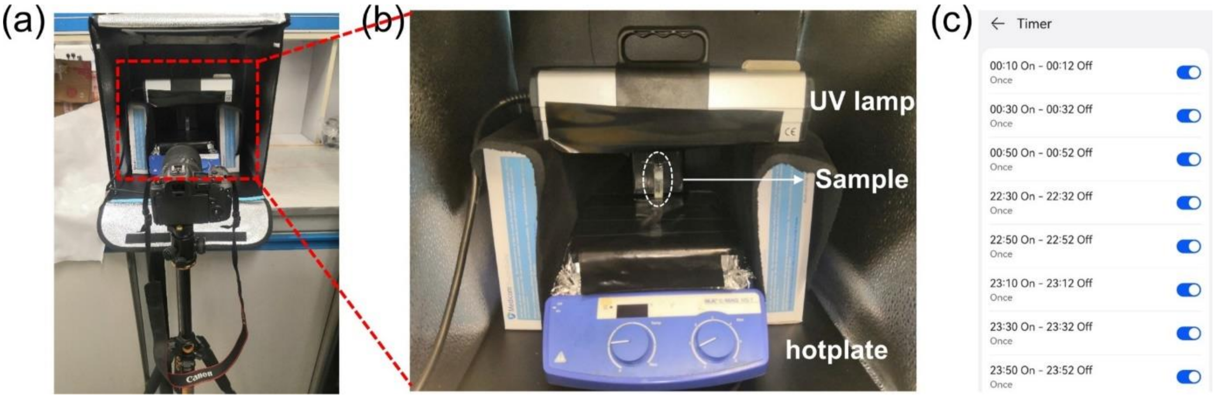

00:10 On - 00:12 Off
Once

00:30 On - 00:32 Off
Once

00:50 On - 00:52 Off
Once

22:30 On - 22:32 Off
Once

22:50 On - 22:52 Off
Once

23:10 On - 23:12 Off
Once

23:30 On - 23:32 Off
Once

23:50 On - 23:52 Off
Once

Figure S5. The experimental setup for controllably taking real-time fluorescent images under 365 nm UV light illumination.

Figure S6. Time-dependent fluorescent images of the TPE-BMO/HDI solution during the curing reaction of HDI with water. The fluorescent images were taken under 365 nm UV light illumination.

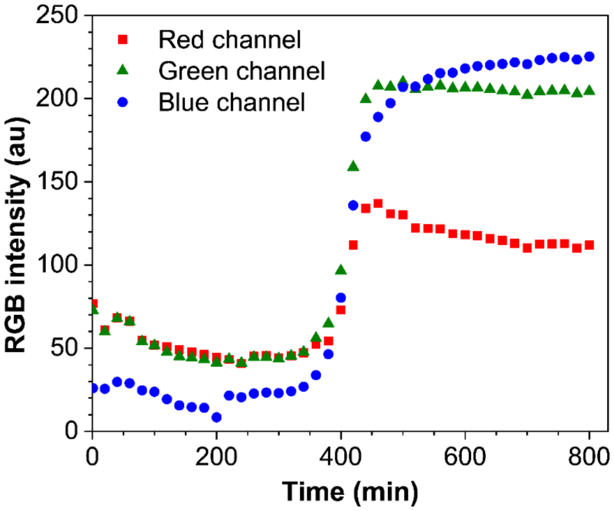

Figure S7. RGB channel intensity as a function of time for the fluorescence images of the TPE-BMO/HDI solution during the curing reaction of HDI with water.

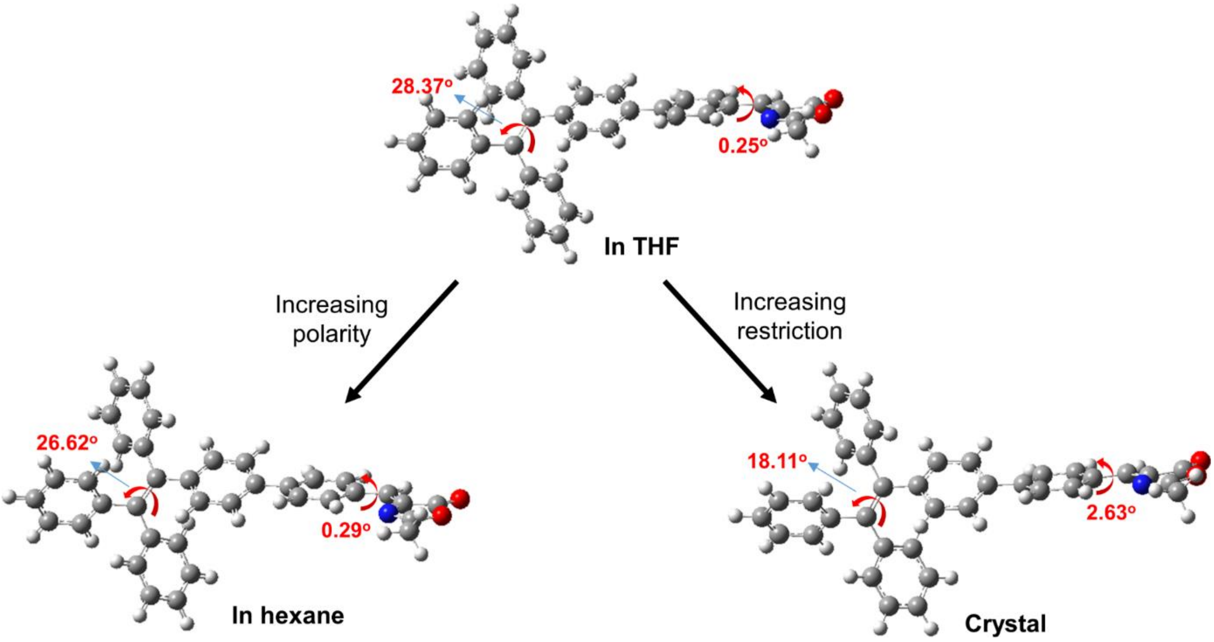

Figure S8. Optimized excited state (S_1) geometries of TPE-BMO in hexane and THF calculated at TD-B3LYP/6-31G(d,p) level and the conformation of the TPE-BMO crystals.

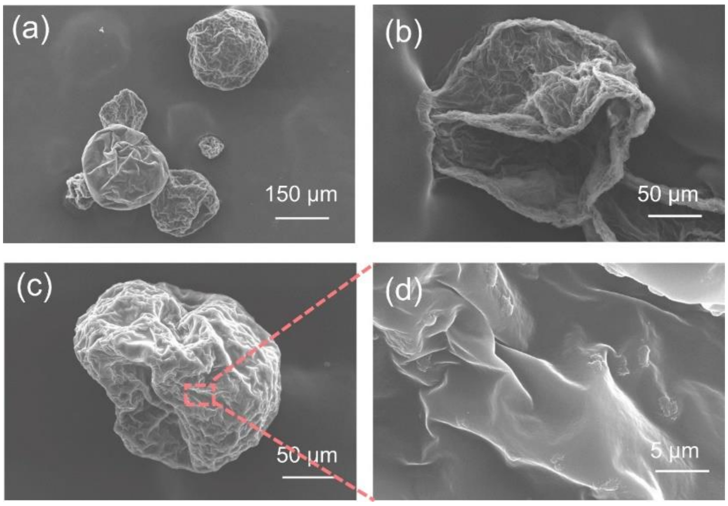

Figure S9. SEM images of PU MCs: (a) an overview of MCs, (b) a ruptured MC, (c) an individual MC, and (d) the enlarged outer surface.

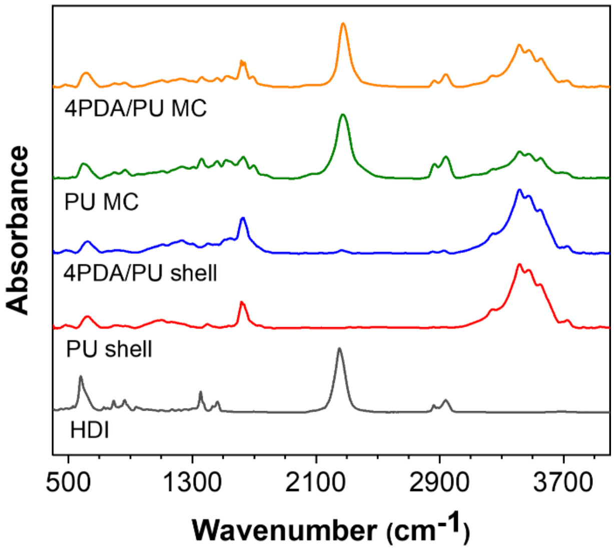

Figure S10. FTIR spectra of HDI, PU shell, 4PDA/PU shell, PU MCs, and 4PDA/PU MCs.

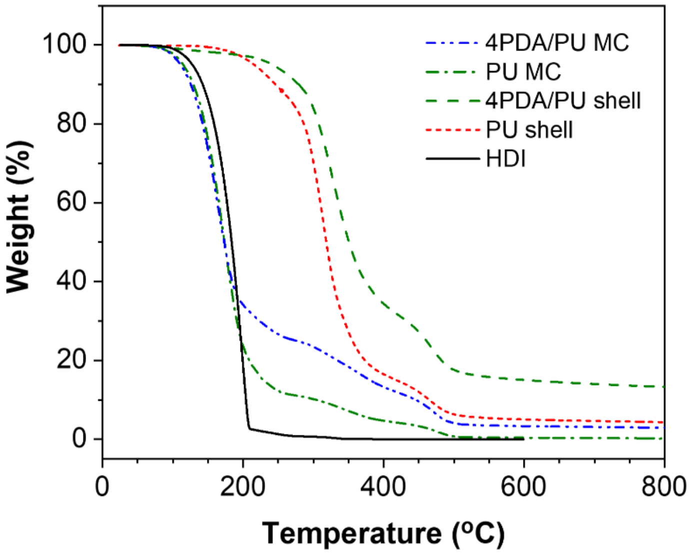

Figure S11. TGA curves of HDI, PU shell, 4PDA/PU shell, PU MCs, and 4PDA/PU MCs.

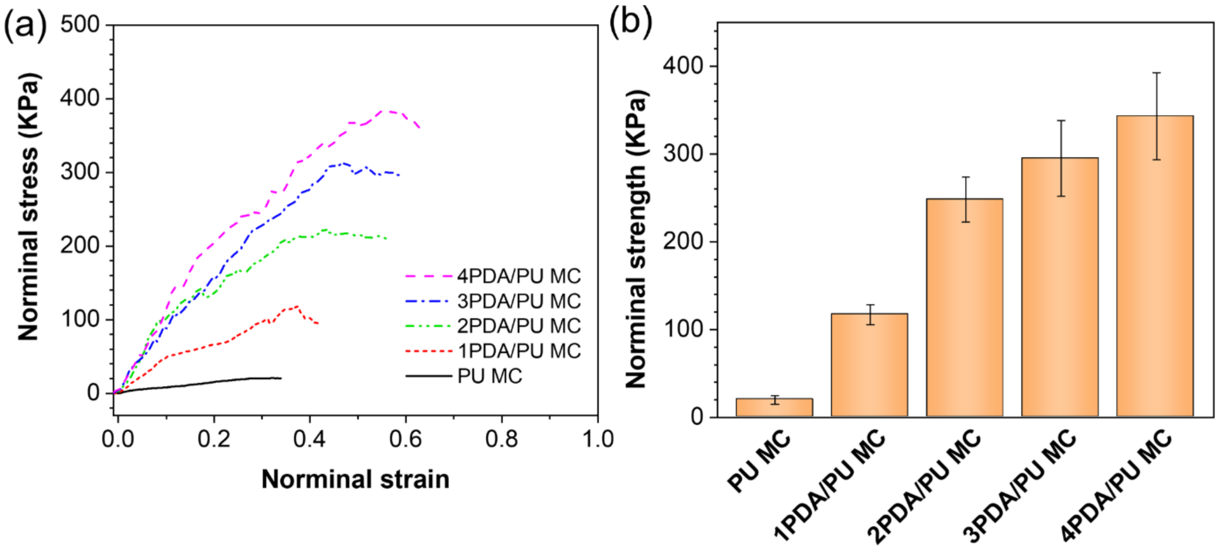

Figure S12. (a) Typical nominal stress-strain curves and (b) nominal strength of PU MCs, 1PDA/PU MCs, 2PDA/PU MCs, 3PDA/PU MCs, and 4PDA/PU MCs.

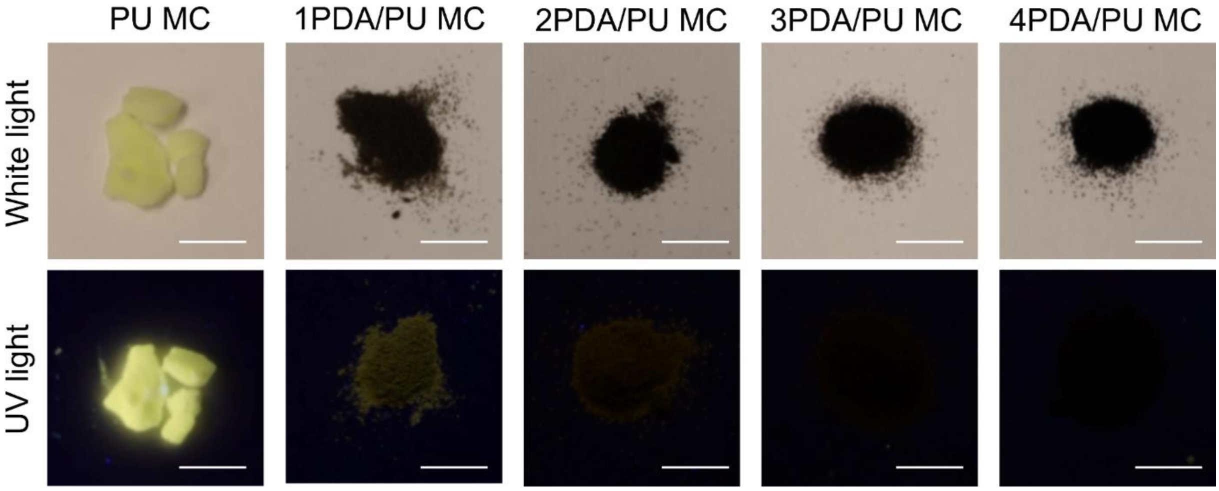

Figure S13. Photographs of PU MCs, 1PDA/PU MCs, 2PDA/PU MCs, 3PDA/PU MCs, and 4PDA/PU MCs taken under room light (upper panel) and 365 nm UV light illumination (lower panel). The scale bar indicates 10 mm.

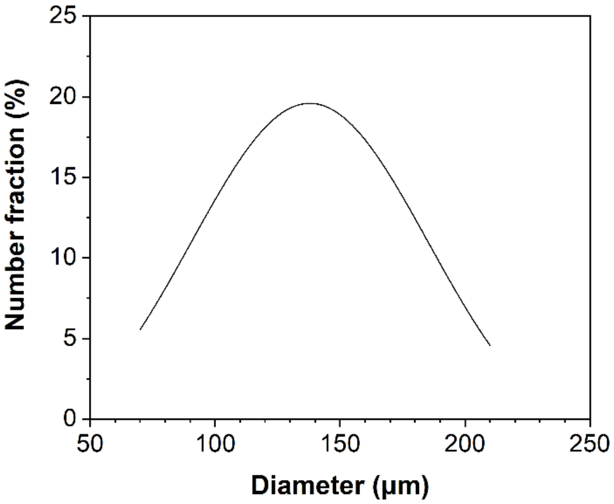

Figure S14. Size distribution of the 4PDA/PU MCs (diameter$_{\text{4PDA/PU MCs}}$ = 140 ± 37 μm).

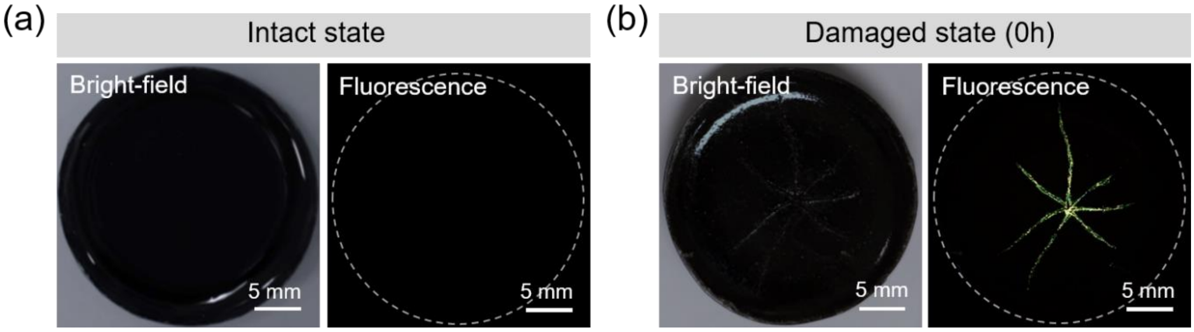

Figure S15. Photographs of (a) the intact MC-embedded EP sample and (b) its damaged sample taken under room light (left) and 365 nm UV light (right).

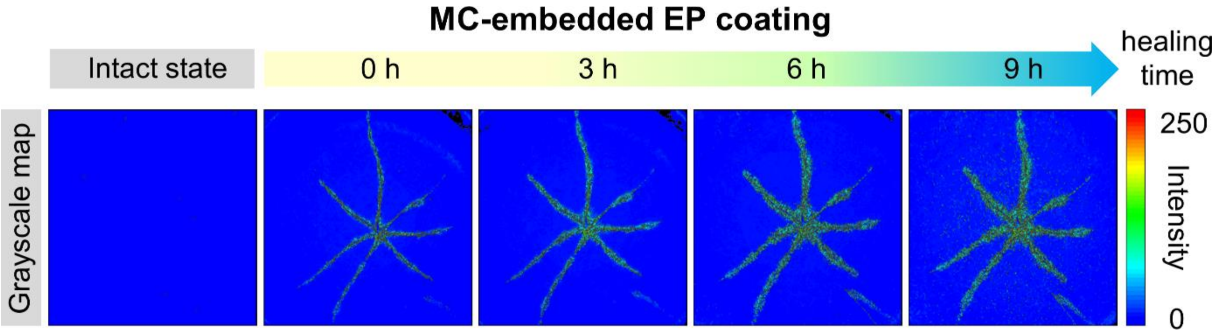

Figure S16. Grayscale analysis of the fluorescent images of the MC-embedded EP coating in the intact state and damaged states at different healing time.